

Defect and anisotropic gap induced quasi-one-dimensional modulation of local density of states in $\text{YBa}_2\text{Cu}_3\text{O}_{7-\delta}$

Khee-Kyun Voo¹, Hong-Yi Chen², and W. C. Wu³

¹*Department of Physics, National Tsing-Hua University, Hsinchu 30043, Taiwan*

²*Texas Center for Superconductivity and Department of Physics, University of Houston, Houston, TX 77204, USA*

³*Department of Physics, National Taiwan Normal University, Taipei 11650, Taiwan*

(November 30, 2002)

Motivated by recent angle-resolved photoemission spectroscopy (ARPES) measurement that superconducting $\text{YBa}_2\text{Cu}_3\text{O}_{7-\delta}$ (YBCO) exhibits a $d_{x^2-y^2}+s$ -symmetry gap, we show possible quasi-one-dimensional modulations of local density of states in YBCO. These anisotropic gap and defect induced stripe structures are most conspicuous at higher biases and arise due to the nesting effect associated with a Fermi liquid. Observation of these spectra by scanning tunneling microscopy (STM) would unify the picture among STM, ARPES, and inelastic neutron scattering for YBCO.

PACS numbers: 74.70.Pq, 74.20.Rp, 74.25.Ld

After more than one and half decades of the discovery of high-temperature superconductors, there lies still one central question: are these materials behave like a Fermi liquid? Recent scanning tunneling measurements (STM) however have provided a new platform in detecting this critical issue, to which modulations of local density of states (LDOS) are observed in superconducting state of $\text{Bi}_2\text{Sr}_2\text{CaCu}_2\text{O}_8$ (BSCCO) [1–3]. More recently, experimentilists managed to obtain Fourier transform (FT) of these LDOS modulations, which then can be immediately used to test whether the system is Fermi-liquid like.

Analogous to angular resolved photo-emission spectroscopy (ARPES), FT-STM can study electronic properties connected to entire Brillouin zone of the system. When a system behaves as a Fermi liquid, Fermi surface (FS) scattering should be clearly identified in normal state. While in superconducting state, it should also give information on how the symmetry of Cooper pair order parameter develops on the FS. Assuming the effect of defect, experimentally observed STM LDOS modulation can be ascribed to quantum interference arising because quasiparticles are scattered by the defect locally. The occurrence of peaks and their evolution as the bias change in the FT-STM spectra seem to be explained well by Fermi liquid models [4–6], whose FS topology is consistent with previous ARPES results. Moreover, the origin of peak moving in FT-STM is very similar to what of the incommensurate peaks observed in inelastic neutron scattering (INS) [7]. Apparently this scenario is in great contrast to the stripe picture [8], interpreted in the STM data of Howald *et al.* [2] and the one-dimensional (1D) INS data of Mook *et al.* [9].

Perhaps of technical involvement, the STM data done for YBCO so far have been limited to the CuO chain layers only [10]. It becomes naturally to ask what would be seen by STM on CuO_2 plane layers of YBCO. As is well known, due to the coupling to the 1D CuO chains, the CuO_2 plane is orthorhombic rather than tetragonal. The perfect D_{4h} symmetry is broken which accounts naturally for the additional symmetry mixed in the order param-

eter of the CuO_2 plane. In this regard, it is commonly accepted that there is a subdominant s -wave component in addition to the dominant $d_{x^2-y^2}$ -wave superconducting gap for CuO_2 planes. This view is supported by earlier tunneling data [11] and verified by recent data of ARPES [12]. The 1D like incommensurate INS peaks [9] can also be interpreted by this picture associated with a Fermi liquid [13]. When fitted to a simple $d_{x^2-y^2}+s$ model, ARPES data reveals that the s -wave component is about 20 % of d -wave component [12].

Here, based on a Fermi liquid model, we investigate the LDOS specific to CuO_2 planes of superconducting YBCO. Similar to other theoretical works [4–6], we consider the effect of defect, while pay special attention to the gap anisotropy. Our goal is to bring out the most conspicuous features and inspire STM measurements to be performed. Successful observation of our predictions in either real-space or FT LDOS could unambiguously identify (1) the goodness of Fermi-liquid behavior and (2) the $d_{x^2-y^2}+s$ symmetry of gap for YBCO. Furthermore this could lead to a unified picture among ARPES [12], INS [9], and STM on YBCO.

To investigate the LDOS spectra, we start by considering the following Hamiltonian

$$H = H_{\text{BCS}} + H_{\text{I}}, \quad (1)$$

where the usual BCS part is

$$H_{\text{BCS}} = \sum_{\mathbf{k}, \sigma} \xi_{\mathbf{k}} c_{\mathbf{k}\sigma}^\dagger c_{\mathbf{k}\sigma} + \sum_{\mathbf{k}} \left[\Delta_{\mathbf{k}} c_{\mathbf{k}\uparrow}^\dagger c_{-\mathbf{k}\downarrow}^\dagger + \text{H.c.} \right] \quad (2)$$

and the part associated with the presence of one single extended impurity located at site 0 is

$$H_{\text{I}} = \sum_{\langle i,j \rangle, \sigma} \delta t_{ij} c_{i\sigma}^\dagger c_{j\sigma} + \sum_{\langle i,j \rangle} \left[\delta \Delta_{ij} c_{i\uparrow}^\dagger c_{j\downarrow}^\dagger + \text{H.c.} \right] + V_0 \left(c_{0\uparrow}^\dagger c_{0\uparrow} + c_{0\downarrow}^\dagger c_{0\downarrow} \right). \quad (3)$$

The parameter δt corresponds to local deviation of hopping due to impurity, $\delta \Delta$ corresponds to local devi-

ation of pairing gap due to impurity, and V_0 is spin-independent impurity potential. Any spin-dependent impurity potential ignoring spin-flip will have no effect in the lowest-order approximation. For extensive but weak impurity scattering, we consider local deviations to those terms $(\delta t_1, \delta \Delta_1)$ couple the impurity site and its nearest neighbors and terms $(\delta t_2, \delta \Delta_2)$ couple impurity's nearest neighbors and next nearest neighbors. Similar kinds of Hamiltonian have been successfully used by Tang and Flatté [4] to explain the resonant STM spectra for Ni impurities in BSCCO and by Wang and Lee [5] and Zhang and Ting [6] to explain the energy-dependent modulation of FT-STM spectra on BSCCO. We shall comment how our results are modified and their experimental relevance when more than one defect are present later.

The local density of states measured by STM is given by

$$D(\mathbf{r}, \omega) = -\frac{1}{2\pi} \text{Im}[G_{11}(\mathbf{r}, \mathbf{r}, \omega + i0^+) - G_{22}(\mathbf{r}, \mathbf{r}, -\omega - i0^+)], \quad (4)$$

where G_{ij} is the element of the 2×2 equal-location single-particle Green's function matrix \hat{G} in Nambu representation. The full \hat{G} can be calculated via the usual Gor'kov-Dyson equation

$$\hat{G}(\mathbf{r}, \mathbf{r}, \omega) = \hat{G}^0(\mathbf{r}, \mathbf{r}, \omega) + \sum_{\mathbf{r}', \mathbf{r}''} \hat{G}^0(\mathbf{r}, \mathbf{r}', \omega) \hat{T}(\mathbf{r}', \mathbf{r}'', \omega) \times \hat{G}^0(\mathbf{r}'', \mathbf{r}, \omega), \quad (5)$$

where $\hat{G}^0(\mathbf{r}_i, \mathbf{r}_j) \equiv \hat{G}^0(\mathbf{r}_i - \mathbf{r}_j)$ correspond to the no-defect ones of $\hat{G}(\mathbf{r}_i, \mathbf{r}_j)$ and the sums (and the T -matrix $\hat{T}(\mathbf{r}', \mathbf{r}'', \omega)$) in Eq. (5) are over the sites associated with H_1 in Eq. (3). For weak impurity scattering, we shall calculate \hat{G} in Eq. (5) up to first order of δt 's, $\delta \Delta$'s, and V_0 , *i.e.*, in the Born limit or first order T -matrix approximation [6]. In our calculation, we use a 800×800 square lattice sites and the impurity is located in the center. For simple but reasonable reason, we choose $2\delta t_1 = 4\delta t_2 = -2\delta \Delta_1 = -4\delta \Delta_2 = V_0$ and assume these scales are small such that the first order T -matrix approximation is valid. It should be emphasized that the weak impurity scattering limit is enough to bring out essential physics. Strong impurity is not expected to give qualitatively new feature away from its neighborhood of interest (see later). For $\xi_{\mathbf{k}}$, we use a tight-binding band $\xi_{\mathbf{k}} = t_1(\cos k_x + \cos k_y)/2 + t_2 \cos k_x \cos k_y + t_3(\cos 2k_x + \cos 2k_y)/2 + t_4(\cos 2k_x \cos k_y + \cos k_x \cos 2k_y)/2 + t_5 \cos 2k_x \cos 2k_y$ (lattice constant $a \equiv 1$), with $t_{1-5} = -0.60, 0.16, -0.05, -0.11, 0.05$ eV respectively for YBCO. The fine structure of the band do not alter the main results reported in this paper. For superconducting gap of YBCO, we assume $\Delta_{\mathbf{k}} = \Delta_d/2(\cos k_x - \cos k_y) + \Delta_s$ with $\Delta_d = 36.7$ meV and $\Delta_s/\Delta_d \equiv s = 0.2$. This gives the maximum gaps at antinodes $(\pi, 0)$ and $(0, \pi)$, $\Delta_{\max}^x = 44$ meV and $\Delta_{\max}^y = 29.3$ meV. Thus $\Delta_{\max}^x/\Delta_{\max}^y = 1.5$ in accordance with ARPES measure-

ment [12]. In our calculation, we also introduce a finite lifetime broadening $\gamma = 2$ meV to the quasiparticle Green's function to smooth our data points by replacing $\omega + i0^+$ with $\omega + i\gamma$.

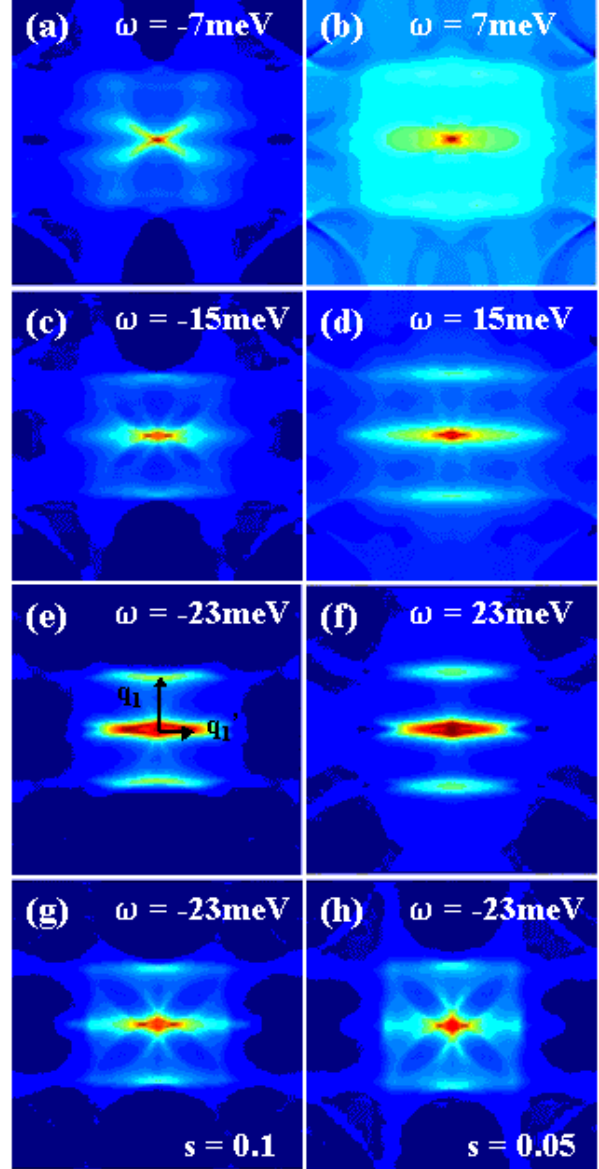


FIG. 1. Bias energy dependent FT-LDOS plotted for the whole first Brillouin zone for a $d_{x^2-y^2} + s$ -wave superconductor. All frames are for anisotropy $s = 0.2$ except for (g) and (h) with $s = 0.1$ and 0.05 , which are intended to be compared to (e). Wavevectors \mathbf{q}_1 and \mathbf{q}'_1 in (e) are the nesting ones shown in Fig. 2.

Theoretically $D(\mathbf{q}, \omega)$, the Fourier transform of $D(\mathbf{r}, \omega)$ is more readily obtained. In Fig. 1, we calculate the bias energy dependent $D(\mathbf{q}, \omega)$ over the whole first Brillouin zone. Energies have been taken from -23 meV to 23 meV — a scale less than the maximum gap at antinode $(0, \pi)$ of $\Delta_{\max}^y = 29.3$ meV. All frames are for anisotropy $s = 0.2$

except (g) and (h) with $s = 0.1$ and 0.05 , which are intended to be compared to (e). The case of small s recovers the results of Wang *et al.* [5] and Zhang *et al.* [6] for a pure $d_{x^2-y^2}$ -wave superconductor. When energy is low [case (a) and (b)], only node-to-node scattering is allowed, to which the finite \mathbf{q} interference is not prominent. The most important interference appears to those zero or small \mathbf{q} scatterings, which nevertheless exhibit clear feature of anisotropic gap. When energy is high [case (e) and (f)], in contrast, finite \mathbf{q} interference peaks emerge in addition to the strong interference structure centered at $\mathbf{q} = 0$.

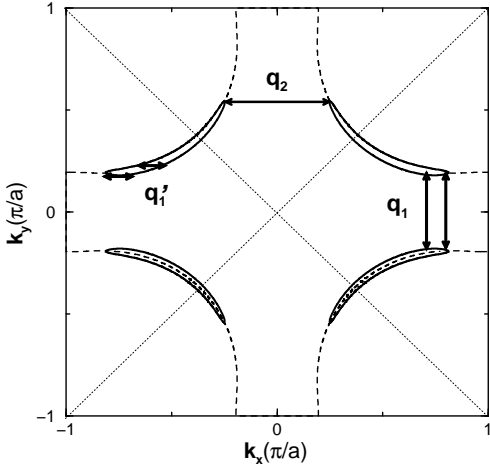


FIG. 2. The Fermi surface (FS) used in our calculation (dash lines) and contours of excitation energy $E_{\mathbf{k}} = 23$ meV (solid lines) are shown. Nesting wavevectors \mathbf{q}_1 and \mathbf{q}'_1 connecting locally almost parallel contours are intimately related to interference peaks. While \mathbf{q}_2 is shown as an example of no associated interference peak. For better visualization, the FS within the upper contours are not plotted.

Fig. 2 shows the Fermi surface used in our calculation, and contours of $E_{\mathbf{k}} = 23$ meV. At this high energy (about half of the maximum gap at antinode $(\pi, 0)$, $\Delta_{\text{max}}^x = 44$ meV), the 2-fold symmetry of the gap causes the contour pair approaching ends of the bananas to be more parallel near x -axis than the pairs near y -axis. The more parallel pair has better nesting effect locally (intra- or inter-contour) [13], which then further enhances the *joint* DOS. In view of Fig. 1(e) or 1(f), conspicuous interference peaks associated with wavevectors \mathbf{q}_1 and \mathbf{q}'_1 are clearly identified (see also Fig. 3). While, for example, no similar interference peak associated with \mathbf{q}_2 (see Fig. 2) is seen.

To illustrate how the \mathbf{q}_1 and \mathbf{q}'_1 peaks evolve as the change of bias energy, we plot $D(\mathbf{q}, \omega)$ in Fig. 3, taking \mathbf{q} along $\mathbf{q}a/\pi = (0,1)-(0,0)-(1,0)$ at bias energy from -5 to -23 meV (left: from bottom to top), and from $+5$ to $+23$ meV (right: from bottom to top). Both frames show clear signatures of \mathbf{q}_1 and \mathbf{q}'_1 peaks which disperse as the bias energy changes. Their intensity increases as bias energy

increases, to which \mathbf{q}_1 disperses convergently to a fixed value near $\pm 0.25(2\pi/a)\hat{y}$, while \mathbf{q}'_1 disperses divergently. No peak develops at \mathbf{q}_2 except some plateaus at intermediate energies. The extensive, centered at zone center $(0, 0)$, quasi-1D like strong interference structure (parallel to k_x axis, see Fig. 3 as well as Fig. 1(e)), comprised of \mathbf{q}'_1 peaks discussed above, is superposed by the zero and small- \mathbf{q} scattering connecting two \mathbf{k} points within the same contour. It is the \mathbf{q}'_1 peaks, which is enhanced by local nesting effect, gives rise to the 1D interference structure parallel to k_x axis.

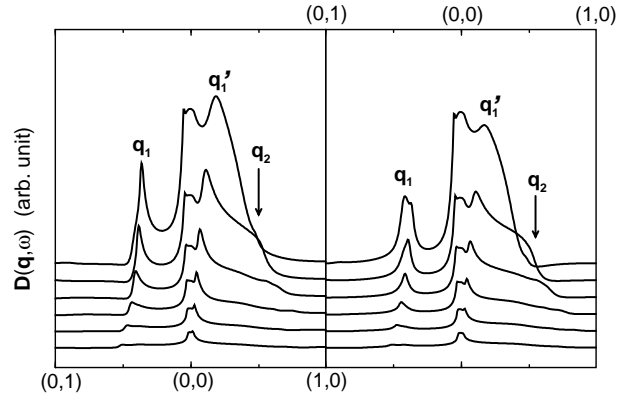


FIG. 3. Scan of $D(\mathbf{q}, \omega)$ (arbitrary units) along $\mathbf{q}a/\pi = (0,1)-(0,0)-(1,0)$ at bias energy from -5 to -23 meV (left: from bottom to top), and from $+5$ to $+23$ meV (right: from bottom to top) at equal energy intervals.

One particular interest on $D(\mathbf{q}, \omega)$ is the *two* \mathbf{q}_1 peaks which have wavevectors near $\pm 0.25(2\pi/a)\hat{y}$. These two peaks, if by themselves alone, would imply a 1D parallel to x -axis stripe pattern in the real-space DOS (with a period of roughly $4a$) — a pattern similar to the phenomenon predicted by “stripe” model [8].

To see how these stripes develop in real-space, in Fig. 4 we present the real-space LDOS modulation, taking Fourier transform of $D(\mathbf{q}, \omega)$. We consider only the $\omega = -23$ meV and $s = 0.2$ case [Fig. 1(e)] and include the $s = 0$ case for comparison. For $s = 0.2$ case, quasi-1D chains of beads of roughly $4a$ wide oriented approximately along x axis are clearly seen at places away from the impurity site. The occurrence of these Friedel-type oscillating stripes arises because of the strong, centered at $(0, 0)$, 1D interference structures. The latter also leads to the variation of intensities along y axis. In contrast, for the four-fold symmetry $s = 0$ case, similar 1D stripes also develop at places away from the impurity site. Clearly there exists no cross stripe pattern (checkerboard) anywhere in the $s = 0$ case, in contradiction to most theoretical predictions [5,6]. Recently Zhang, Hu, and Yu [14] considered the Zn or Ni impurity induced modulations of real-space LDOS for a $d_{x^2-y^2}$ -wave superconductor which has a simple continuum band of circular FS. They [14] re-

ported similar circularly one-dimensional (not cross) patterns.

It should be emphasized that all the experimental \mathbf{q} -space peaks are obtained upon Fourier transforming a single chosen piece of real space, which shows no sign of localized impurities. While in our approach, it is clear that the different \mathbf{q} peaks are originated from different patches of space surrounding the impurity (see Fig. 4). To relate our calculation ($s = 0$ case) to the experiments (checkerboard pattern), we need to have *dilute* impurities, such that the decaying Friedel oscillations emanating from individual impurities overlap crossly at some open spaces, and therefore Fourier transforming this single region gives all the \mathbf{q} peaks.

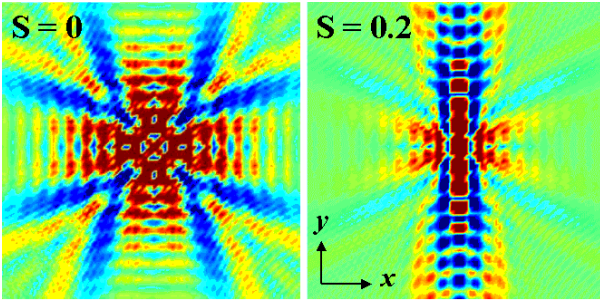


FIG. 4. Modulations of real-space LDOS for bias frequency $\omega = -23$ meV. The left (right) frame is for a $d_{x^2-y^2}+s$ -wave superconductor with $s = 0$ (0.2) and both are presented for $x, y = -40$ to $40a$. Single impurity is located at the center.

A direct consequence of this picture is that when the impurity concentration is too high, the LDOS oscillations will be smoothed out, as the phases of the oscillations will be pinned by individual impurities and therefore *incoherent*. This will be in contrast to the genuine stripe scenario [8] where the oscillation will be expected to be more prominent since the stripes, fluctuating in smooth real spaces, will now get pinned by the impurities.

The case of multiple impurities for BSCCO is recently considered by Morr *et al.* [15] and Zhu *et al.* [16]. Very recently Anderson and Hedegård [17] also study the quantum interference between multiple impurities for a $d_{x^2-y^2}$ -wave superconductor, whose pairing state could become $d_{x^2-y^2} + id_{xy}$ or $d_{x^2-y^2} + is$ -wave at some doping level. Our dilute multi-impurity regime discussed above is fundamentally different from that any one else [15–17] has studied. Let the length scale between the impurities be d_0 , and the distance away from the impurities, where we are interested, be d . Our interesting regime is then $d_0 \sim d \gtrsim 20a$ (see Fig. 4), while the case other people have studied was $d_0 \sim d \sim$ a few a .

Finally one does not expect any qualitatively new physics at the use of an unitary impurity, since it is known to affect only the LDOS locally close to the impurities, whereas we are now most interested in the regions away from the impurities. The essential point is that impurity

scatters the quasiparticles, no matter in Born or unitary limit.

In summary, motivated by recent ARPES and INS results which are consistent with the picture that YBCO has superconducting gap of $d_{x^2-y^2}+s$ symmetry, we predict that quasi-one-dimensional Friedel-type stripes can be induced by defect in superconducting YBCO, observable by STM measurement. This phenomenon is most conspicuous at higher biases and associated with the local nesting effect for a Fermi liquid. Hopefully the predicted modulations in either real or Fourier space can be tested by STM measurement soon.

This work is supported by National Science Council of Taiwan under Grant No. 91-2112-M-003-020.

-
- [1] J.E. Hoffman, E.W. Hudson, K.M. Lang, V. Madhavan, H. Eisaki, S. Uchida, J.C. Davis, *Science* **295**, 466 (2002).
 - [2] C. Howald, H. Eisaki, N. Kaneko, and A. Kapitulnik, *cond-mat/0201546*.
 - [3] J.E. Hoffman, K. McElroy, D.H. Lee, K.M. Lang, H. Eisaki, S. Uchida, J.C. Davis, *Science* **297**, 1148 (2002).
 - [4] J.-M. Tang and M.E. Flatté, *Phys. Rev. B* **66**, 060504 (2002).
 - [5] Q.-H. Wang and D.H. Lee, *cond-mat/0205118*.
 - [6] D. Zhang and C.S. Ting, *cond-mat/0209318*.
 - [7] P. Bourges, Y. Sidis, H.F. Fong, L.P. Regnault, J. Bossy, A. Ivanov, and B. Keimer, *Science* **288**, 1234 (2000).
 - [8] S.A. Kivelson *et al.*, *cond-mat/0210683*.
 - [9] H.A. Mook, P. Dai, F. Dogan, and R.D. Hunt, *Nature* **404**, 729 (2000).
 - [10] D.J. Derro, E.W. Hudson, K.M. Lang, S.H. Pan, J.C. Davis, J.T. Markert, and A.L. de Lozanne, *Phys. Rev. Lett.* **88**, 097002 (2002).
 - [11] A.G. Sun, D.A. Gajewski, M.B. Maple, and R.C. Dynes, *Phys. Rev. Lett.* **72**, 2267 (1994).
 - [12] D.H. Lu, D.L. Feng, N.P. Armitage, K.M. Shen, A. Damascelli, C. Kim, F. Ronning, Z.-X. Shen, D.A. Bonn, R. Liang, W.N. Hardy, A.I. Rykov, and S. Tajima, *Phys. Rev. Lett.* **86**, 4370 (2001).
 - [13] K.K. Voo, H.Y. Chen, and W.C. Wu, *Physica C* **382**, 323 (2002).
 - [14] G.-M. Zhang, H. Hu, and L. Yu, *Phys. Rev. B* **66**, 104511 (2002).
 - [15] D.K. Morr and N.A. Stavropoulos, *Phys. Rev. B* **66**, 140508(R) (2002).
 - [16] L. Zhu, W.A. Atkinson, and P.J. Hirschfeld, *cond-mat/0208008*.
 - [17] B.M. Anderson and P. Hedegård, *cond-mat/0301225*.